# Preparation, Spectroscopic Properties, and Crystal Structures of $Fe_2(CO)_6(\mu\text{-}CO)(\mu\text{-}CF_2)_2$, $Fe_2(CO)_6(\mu\text{-}CO)_2(\mu\text{-}CF_2)$, and $Fe_2(CO)_6(\mu\text{-}CF_2)(PPh_3)_2$ – Theoretical Studies of Methylenic *vs.* Carbonyl Bridges in Diiron Complexes

**W. Petz*,[a], F. Weller[a], A. Barthel[b], C. Mealli[c], and J. Reinhold**,[b]**

[a] Marburg, Fachbereich Chemie der Philipps-Universität
[b] Leipzig, Wilhelm-Ostwald-Institut für Physikalische und Theoretische Chemie der Universität
[c] Firenze/Italy, Istituto per lo Studio della Stereochimica ed Energetica dei Composti di Coordinazione, CNR

Received April 27th, 2001.

*Ad memoriam Egon Wiberg*

**Abstract.** The reaction of $Na_2[Fe(CO)_4]$ with $Br_2CF_2$ in n-pentane generates a mixture of the compounds $(CO)_3Fe(\mu\text{-}CO)_{3-n}(\mu\text{-}CF_2)_nFe(CO)_3$ (**2**, n = 2; **3**, n = 1) in low yields with **3** as the main product. **3** is obtained free from **2** by reacting $Br_2CF_2$ with $Na_2[Fe_2(CO)_8]$. The non-isolable monomeric complex $(CO)_4Fe{=}CF_2$ (**1**) can probably considered as the precursor for **2**. **3** reacts with $PPh_3$ with replacement of two CO ligands to form $Fe_2(CO)_6(\mu\text{-}CF_2)(PPh_3)_2$ (**4**). The complexes **2**–**4** were characterized by single crystal X-ray diffraction. While the structure of **2** is strictly similar to that of $Fe_2(CO)_9$, the structure of **3** can better be described as a resulting from superposition of the two enantiomers **3a** and **3b** with two semibridging CO groups. Quantum chemical DFT calculations for the series $(CO)_3Fe(\mu\text{-}CO)_{3-n}(\mu\text{-}CF_2)_nFe(CO)_3$ (n = 0, 1, 2, 3) as well as for the corresponding $(\mu\text{-}CH_2)$ derivatives indicate that the progressively larger $\sigma$ donor and $\pi$ acceptor properties for the bridging ligands, in the order $CO < CF_2 < CH_2$, favor a stronger Fe–Fe bond.

**Keywords:** Iron carbonyl; Carbondifluoride ligand; DFT calculations; Crystal structure

# Darstellung, spektroskopische Eigenschaften und Kristallstrukturen von $Fe_2(CO)_6(\mu\text{-}CO)(\mu\text{-}CF_2)_2$, $Fe_2(CO)_6(\mu\text{-}CO)_2(\mu\text{-}CF_2)$ und $Fe_2(CO)_6(\mu\text{-}CF_2)(PPh_3)_2$ – Theoretische Untersuchung über Methylen- *vs.* Carbonyl-Brücken in Dieisen Komplexen

**Inhaltsübersicht.** Aus der Reaktion von $Na_2[Fe(CO)_4]$ mit $Br_2CF_2$ in n-Pentan läßt sich ein Gemisch der Komplexe $(CO)_3Fe(\mu\text{-}CO)_{3-n}(\mu\text{-}CF_2)_nFe(CO)_3$ (**2**, n = 2; **3**, n = 1) in mäßigen Ausbeuten isolieren, wobei **3** das Hauptprodukt ist. Man erhält **3** auch frei von **2** bei der Umsetzung von $Br_2CF_2$ mit $Na_2[Fe_2(CO)_8]$. Der nicht isolierbare monomere Komplex $(CO)_4Fe{=}CF_2$ (**1**) ist vermutlich als Vorstufe für **2** aufzufassen. **3** reagiert mit $PPh_3$ unter Verdrängung von zwei CO-Liganden zu $Fe_2(CO)_6(\mu\text{-}CF_2)(PPh_3)_2$ (**4**) ab. Die Komplexe **2**–**4** sind durch Kristallstrukturanalysen charakterisiert. Während die Struktur von **2** der von $Fe_2(CO)_9$ ähnlich ist, läßt sich die von **3** besser als Überlagerung der Enantiomeren **3a** und **3b** mit zwei halbverbrückenden CO-Gruppen beschreiben. Quantenchemische DFT-Rechnungen für die Reihe $(CO)_3Fe(\mu\text{-}CO)_{3-n}(\mu\text{-}CF_2)_nFe(CO)_3$ (n = 0, 1, 2, 3) sowie für die entsprechenden $(\mu\text{-}CH_2)$-Verbindungen zeigen, daß die fortschreitend stärkeren $\sigma$-Donor- und $\pi$-Acceptoreigenschaften der Brückenliganden in der Reihe $CO < CF_2 < CH_2$ eine stärkere Fe–Fe-Bindung favorisieren.

* Prof. Dr. Wolfgang Petz
Fachbereich Chemie der Philipps-Universität
D-35032 Marburg
Fax: ++49-64 21-2 82 56 53
E-mail: petz@mailer.uni-marburg.de
** Prof. Dr. Joachim Reinhold
Wilhelm Ostwald-Institut für Physikalische und Theoretische Chemie der Universität Leipzig
D-04103 Leipzig
Fax: ++49-3 41-9 73 63 99
E-mail: reinhold@quant1.chemie.uni-leipzig.de

## Introduction

Transition metal complexes with the difluorocarbene ligand, $CF_2$, are known since many years and an excellent review has appeared summarizing the relevant preparative and theoretical studies on this field of chemistry [1]. Similar to CO and some related alkylidenes the $CF_2$ ligand is coordinated either in a terminal or in a bridging manner. Terminal $CF_2$ complexes concentrate on compounds of molybdenum, the iron triad, and iridium. A few complexes with the $CF_2$ li-

gand bonded in a bridging manner are known from manganese [2], iron [3], cobalt, and iridium [2, 3]. It was concluded, that dihalogencarbene complexes are links between the typical heteroatom stabilized electrophilic "Fischer" carbene complexes and the nucleophilic alkylidene compounds of the "Schrock" type. Thus, depending on the further substituents and the oxidation state of the central metal atom, the coordinated $CF_2$ ligand exhibits nucleophilic or electrophilic behavior. The ground state of the free $CF_2$ ligand is a singlet [4] similar to that of heteroatom stabilized carbenes, while the ground state of alkylidenes is a triplet state [5].

The access to difluorocarbene complexes with a terminal ligand follows two main pathways. One route starts from the corresponding transition metal $CF_3$ complexes reacting with fluoride abstracting agents. The other route comprises transfer of $CF_2$ from $M(CF_3)_2$ (M = Hg, Cd) to low valent transition metal compounds [1]. In one case the thermal decomposition of a complex with the $Ir(COCF_2Cl)$ fragment leads to the formation of the corresponding $CF_2$ complex [6].

Compounds with a bridging $CF_2$ ligand originate from various sources including the cheap and easily available dibromodifluoromethane. This compound is well known in organic chemistry to generate the difluorocarbene species by reacting with elemental lead [7, 8] and was also reported to react with neutral carbonyl compounds of Co and Fe under photochemical conditions to produce $\mu$-$CF_2$ complexes [3].

This paper describes the access to the compounds $Fe_2(CO)_7(\mu\text{-}CF_2)_2$, $Fe_2(CO)_8(\mu\text{-}CF_2)$ and $Fe_2(CO)_6(\mu\text{-}CF_2)(PPh_3)_2$ using $Br_2CF_2$ as $CF_2$ source [9]. Furthermore, theoretical studies of the series of compounds of the type $(CO)_3Fe(\mu\text{-}CO)_{3-n}(\mu\text{-}CF_2)_nFe(CO)_3$ (n = 1, 2, 3) are presented in comparison to the corresponding ($\mu$-$CH_2$) compounds.

## Results and Discussion

### 1 Preparation

Addition of an excess of $Br_2CF_2$ to a suspension of Collmans reagent in n-pentane leads to a slight warming of the mixture and formation of a dark greenish brown solution and a dark brown to black solid. A mixture of the compounds **2** and **3** is isolated from the residue of the pentane solution upon sublimation. The formation of both compounds during the reaction can be rationalized from the following reactions summarized in scheme 1.

The expected monomeric species **1** could not be isolated; however, the presence of **2** is an indirect proof for the formation of **1** being formed in the first step of the reaction. **1** is probably unstable under the reaction conditions and reacts either with itself to give **2** or with $Fe(CO)_5$ to produce additional amounts of **3**. An-

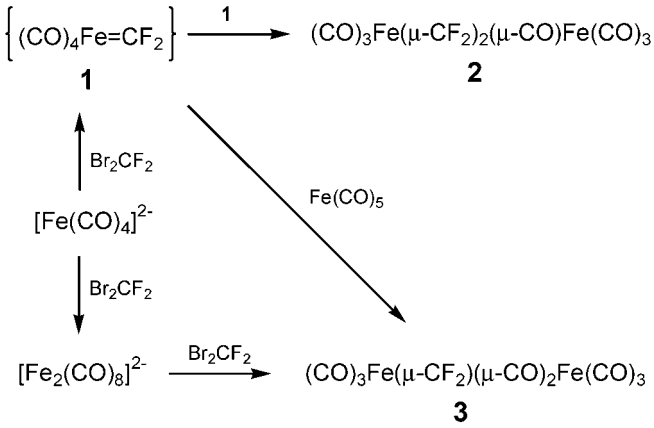


**Scheme 1**

other source for **2** would be the reaction of $Br_2CF_2$ with a reduced species of **3**, but we were not able to increase the yield of **2** upon reducing **3** and again reacting with $Br_2CF_2$.

We suppose, that $Br_2CF_2$ acts not only as a source for $CF_2$ but also as an oxidizing reagent towards the dianion $[Fe(CO)_4]^{2-}$. The oxidation (geminal dihalides such as $Br_2CF_2$, $Cl_2CS$ or even $Cl_2CH_2$ often mimic halogen) generates first $[Fe_2(CO)_8]^{2-}$ which also produces **3** with $Br_2CF_2$ so that **3** is the main product. $Fe(CO)_5$ always forms when polynuclear carbonylates of iron are exposed to oxidizing agencies.

While **3** is the main product, the portion of **2** amounts only about 5% and the overall yield of the mixture varies between 12 and 23%. The material is separated by vacuum sublimation or by low temperature crystallization from n-pentane. The complex **3** is obtained free from **2** if the reaction is carried out under similar conditions with $Na_2[Fe_2(CO)_8]$; the corresponding Li-salt [10] leads to the same results. So we believe, that the dianion is the main source for the formation of **3**.

The choice of the solvent is very important for reaction and isolation. Thus, if the reaction is carried out in THF solution only traces of **2** and **3** are formed as shown by $^{19}F$ NMR spectroscopy. $Br_2CF_2$ as solvent, however, leads to the same results as found in n-pentane solution. The relative amounts of **2** and **3** are independent of the reaction temperature and do also not change upon reverse addition of the educts. Below –20 °C no reaction is observed; it starts above this temperature indicating by forming a brownish solution. Attempts to separate **2** and **3** by column chromatography have failed.

Two of the carbonyl groups of **3** can be replaced by phosphine ligands. If a pentane solution of **3** is added at room temperature to a solution of two equivalents of $PPh_3$ in n-pentane immediately brown crystals of **4** begin to separate, and within a few minutes quantitative yield is obtained. The crystals were directly suitable for X-ray analysis.

$$\mathbf{3} + 2\,PPh_3 \rightarrow (CO)_3(Ph_3P)Fe(\mu\text{-}CF_2)Fe(PPh_3)(CO)_3 + 2\,CO \quad (1)$$
$$\mathbf{4}$$

**4** is stable as a solid under an argon atmosphere but unstable in solution; in THF or in toluene slow decomposition occurs to produce $(CO)_3Fe(PPh_3)_2$ along with traces of $(CO)_4FePPh_3$ (see spectroscopic results). Attempts to prepare **4** in THF or toluene lead to a mixture of **4** with the tri- and tetracarbonyl iron phosphine compounds. The remaining of the $CF_2$ group could not yet be cleared up (see $^{19}F$ NMR spectroscopy).

Other phosphines such as $P(NMe_2)_3$ or dppe also react with **3**, but the isolated products are not totally characterized as yet. Attempts to reduce **3** with alkali metals have failed. Further studies on the chemistry of **2** and **3** are presently in progress.

## 2 Spectroscopy

The infrared spectrum of **2** exhibits strong bands in the typical region for terminal CO groups and one sharp and intense band at 1879 $cm^{-1}$ which can be assigned to the single bridging carbonyl ligand. Two medium intense bands at 1091 and 1046 $cm^{-1}$ belong to stretching vibrations of the $CF_2$ group. The IR spectrum of **3** does not clearly announce the presence of bridging CO ligands; the bands of the terminal CO groups are only accompanied by a shoulder on the low frequency side of the carbonyl bands, which can be attributed to semibridging CO groups and the appearance of the bands is independent from the polarity of the solvent. The $\nu$(CF) vibrations of **3** are shifted to 1034 and 997 $cm^{-1}$. High values of the $\nu$(CO) stretching frequencies in **2** and **3** suggest that the $\pi$-acceptor ability of the $CF_2$ ligand is substantially higher than that of a CO ligand as shown by comparison with the $\nu$(CO) frequencies in $Fe_2(CO)_9$ (2018, 1829 $cm^{-1}$).

The IR spectrum of **4** exhibits only bands of terminal CO groups, the center of which, however, has shifted to lower frequencies relative to the CO vibrations of **2** and **3** according to the more electron donating properties of the phosphines. In the region of the $\nu$(CF) vibrations medium intense bands at 997 and 937 $cm^{-1}$ can be assigned to the $CF_2$ ligand, similarly shifted to lower frequencies like the carbonyl bands.

Relative to matrix isolated free $CF_2$ with the $\nu_s$(FCF) at 1102 and $\nu_{as}$(FCF) at 1221 $cm^{-1}$ the two CF vibrations of the complexes **2** to **4** are shifted to lower frequencies [11] and we suppose that in the complexes similarly the bands at higher frequencies can be assigned to the asymmetric $CF_2$ vibration.

The $CF_2$ ligand is easily characterized by $^{19}F$ and $^{13}C$ NMR spectroscopy. While terminal ligands exhibit strongly deshielded fluorine and carbon atoms with shifts to about 160 (F) and 270 (C) ppm [12, 13] a shift to higher field is observed for both nuclei when arranged in a bridge. The $^{19}F$ NMR spectrum of **2** displays two doublets at 61 and 22 ppm according to fluorine atoms in different chemical environments; the fluorine atoms of **3** produces a singlet at 51 ppm. In the $^{13}C$ NMR spectrum of **3** the $CF_2$ carbon atom appears at 219 ppm with $^1J_{C,F} = 384$ Hz typical for bridging $CF_2$ ligands [2, 3, 14]. The CO groups of **3** exhibit a single resonance which, at –40 °C splits into a triplet due to the coupling with the fluorine atoms. This indicates scrambling within the NMR time scale. Unfortunately, the spectra could not be recorded at lower temperatures due to the crystallization of the species.

Replacement of two CO groups by $PPh_3$ causes the $^{19}F$ NMR signal in **4** to shift from 51 ppm to 42 ppm indicating a better shielding of the fluorine atoms under the influence of the phosphine ligands. In solution **4** shows highly dynamic behavior; the two differently bonded phosphine ligands give only one $^{31}P$ NMR signal ($J_{P,F} = 8.4$ Hz) and the four chemically different types of CO groups found in the solid state are also condensed to one signal in the solution $^{13}C$ NMR spectrum down to –40 °C. Again, crystallization did not allow to work at lower temperatures. These results indicate a rapid scrambling of the ligands in the NMR time scale but a description of the actuel mechanism can only be speculative at this time. Whether bridging CO or $PPh_3$ groups are involved as intermediates or the scrambling takes place isolated at each iron atom is a still open question.

As mentioned above, solutions of **4** at room temperature are not stable and a slow decomposition is observed with formation of the known complex $(CO)_3Fe(PPh_3)_2$ and less amounts of $(CO)_4FePPh_3$. After about 200 h in THF solution, the original $^{19}F$ NMR signal of **4** has disappeared and new signals appear at 99 (main signal), 52, 47, 7 and –45 ppm. A similar evolution is observed in the $^{31}P$ NMR spectrum which shows signals of the phosphine species along with bands at 63, 49, and 41 ppm. The latter have not been identified as yet.

The slow decomposition of **4** in solution leads to the suggestion that concentration of the phosphine ligands at one iron atom may be an irreversible process leading to splitting off $(CO)_3Fe(PPh_3)_2$. Such an intermediate is probably not involved in the scrambling process.

## 3 Crystal Structures

### *3.1 General remarks*

The structures of the compounds **2**, **3**, and **4** could be confirmed by single-crystal X-ray analyses. Suitable crystals of **2** and **3** were obtained by slow evaporation of the solvent from a solution in n-pentane. Crystals of **4** were obtained by addition of a solution of $PPh_3$ in n-pentane to a solution of **3** in the same solvent. ORTEP views of the molecules are depicted in Figures 1 to 4; details of the structure determination are

**Table 1** Experimental data for the X-ray studies of the complexes **2**, **3** and **4**

| | **2** | **3**[a] | **3**[b] | **4** |
|---|---|---|---|---|
| empirical formula | $C_9F_4Fe_2O_7$ | $C_9F_2Fe_2O_8$ | $C_9F_2Fe_2O_8$ | $C_{43}H_{30}F_2Fe_2O_6P_2$ |
| formula weight | 407.79 | 385.79 | 385.79 | 854.31 |
| crystal size/mm$^3$ | 0.18 × 0.34 × 0.34 | 0.08 × 0.17 × 0.41 | 0.08 × 0.17 × 0.41 | 0.35 × 0.27 × 0.04 |
| crystal system | orthorhombic | monoclinic | monoclinic | triclinic |
| space group | Pnma | $P2_1/m$ | $P2_1/m$ | $P\bar{1}$ |
| unit cell dimensions/pm | a = 895.7(2) | a = 625.9(1) | a = 625.9(1) | a = 1059.2(1) |
| | b = 1113.1(2) | b = 1199.8(2) | b = 1199.8(2) | b = 1361.4(1) |
| | c = 1237.8(4) | c = 847.5(1) | c = 847.5(1) | c = 1436.4(1) |
| | | | | $\alpha$ = 97.113(11) |
| | | $\beta$ = 107.180(10) | $\beta$ = 107.180(10) | $\beta$ = 110.008(11) |
| | | | | $\gamma$ = 93.562(12) |
| Z | 4 | 2 | 2 | 2 |
| $d_c$/gcm$^{-3}$ | 2.195 | 2.107 | 2.107 | 1.478 |
| volume (×10$^{-30}$ m$^3$) | 1234.1(6) | 608.3(1) | 608.0(1) | 1919.1(3) |
| cell determination | | 2000 rflns | 2000 rflns | 8000 rflns |
| temperature/K | 293(2) | 203(2) | 203(2) | 213(2) |
| F(000) | 792 | 376 | 376 | 872 |
| diffractometer | CAD4 (Enraf-Nonius) | IPDS (Stoe) | IPDS (Stoe) | IPDS (Stoe) |
| wave length/pm | 154.178 | 71.073 | 71.073 | 71.073 |
| theta range for data collection | 5.34 to 74.79° | 2.52 to 28.00° | 2.52 to 28.00° | 2.06 to 26.97° |
| index range | 0 < h < 11, –13 < k < 0, | –8 < h < 8, –15 < k < 15, | –8 < h < 8, –15 < k < 15, | –13 < h < 13, –17 < k < 17, |
| | –15 < l < 0 | –10 < l < 11 | –10 < l < 11 | –18 < l < 18 |
| scan method | omega scans | phi-scans | phi-scans | phi-scans |
| control reflections and decay | 2 rfls all 120 min, 0% | | | |
| reflections collected | 1329 | 5544 | 5544 | 21041 |
| independent | 1329 [$R_{int}$ = 0.000] | 1496 [$R_{int}$ = 0.0302] | 1496 [$R_{int}$ = 0.0302] | 7729 [$R_{int}$ = 0.0646] |
| observed [I > 2$\sigma$(I)] | 1121 | 1265 | 1265 | 4253 |
| rfls used for refinement | 1329 | 1496 | 1496 | 7729 |
| completeness | 99.6% (to theta = 74.79°) | 97.3% (to theta = 28.00°) | 97.3% (to theta = 28.00°) | 92.4% (to theta = 26.97°) |
| largest diff. peak and hole | 0.621 and –0.478 e · A$^{-3}$ | 0.701 and –1.442 e · A$^{-3}$ | 0.492 and –0.406 e · A$^{-3}$ | 0.740 and –0.388 e · A$^{-3}$ |
| solution | direct/difmap | direct/difmap | direct/difmap | direct/difmap |
| refinement | full matrix least squares on $F^2$ | full matrix least squares on $F^2$ | full matrix least squares on $F^2$ | full matrix least squares on $F^2$ |
| hydrogen atoms | | | | geom, mixed |
| programs used | SHELXS-97 (Sheldrick, 1990) | SHELXS-97 (Sheldrick, 1990) | SHELXS-97 (Sheldrick, 1990) | SHELXS-97 (Sheldrick, 1990) |
| | SHELXL-97 (Sheldrick, 1997) | SHELXL-97 (Sheldrick, 1997) | SHELXL-97 (Sheldrick, 1997) | SHELXL-97 (Sheldrick, 1997) |
| | SHELXTL | SHELXTL | SHELXTL | SHELXTL |
| data/restraints/parameters | 1329/0/112 | 1496/0/106 | 1496/10/181 | 7729/0/430 |
| goodness-of-fit on $F^2$ | 1.117 | 1.097 | 0.981 | 0.838 |
| R index (all data) | wR2 = 0.1112 | wR2 = 0.1247 | wR2 = 0.0704 | wR2 = 0.1137 |
| R index conventional [I > 2$\sigma$(I)] | R1 = 0.0364 | R1 = 0.0465 | R1 = 0.0273 | R1 = 0.0455 |

[a] refined mediated, [b] refined disordered

collected in Table 1; bond lengths and angles are summarized in Table 3 to 5. Other crystal structures of compounds containing a bridging $CF_2$ ligand have been reported for $(CO)_4Mn(\mu\text{-}CF_2)_2Mn(CO)_4$ [2] and the heterobimetallic complex $[Cp(CO)Fe(\mu\text{-}CF_2)(\mu\text{-}CO)IrCl(CO)(PMe_2Ph)]BF_4$ [14].

### *3.2 Molecular structure of **2***

The structure of **2** is shown in Fig. 1. The molecule can be regarded as a derivative of $Fe_2(CO)_9$ in which two bridging CO groups are replaced by $CF_2$ ligands. The Fe–Fe distance of 247 pm is about 6 pm shorter than in $Fe_2(CO)_9$ [15] and, to our knowledge, is the shortest one found in these types of compounds. A comparison with the average structure of **3** reveals that more $CF_2$ groups in place of the CO ones favor the closeness of the metal atoms (see theoretical part). The single bridging CO ligand along with the metal atoms and two terminal carbonyl groups are located on the crystallographic mirror plane of the molecule.

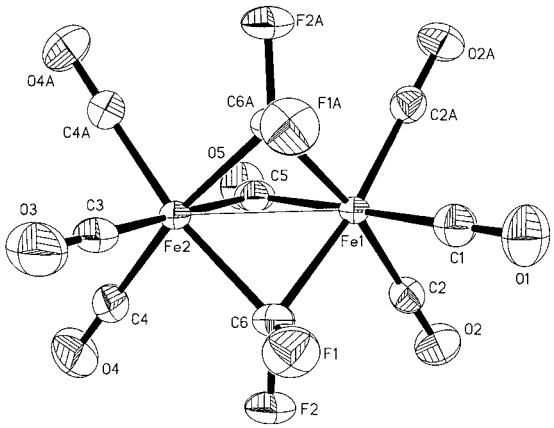


**Fig. 1** Molecular structure of **2** with atomic numbering scheme; thermal ellipsoids are shown at the 50% probability level.

By ignoring the Fe–Fe bond, the coordination of each metal atom is nearly octahedral with the two octahedra sharing one face. The F–C–F angle of 103.9° is

similar to those found in the other two known structures of compounds with bridging $CF_2$ ligands [2, 14].

Surprisingly, the dihedral angle between the planes formed by Fe(1), C(6), and Fe(2) and Fe(1), C(6a), and Fe(2) deviates from 120° (111° is recorded). This might be due to either a repulsion between the bridging CO and $CF_2$ groups or attraction between the $CF_2$ groups themselves. Remarkably, the distance between the F(1) and F(1a) atoms from the different $CF_2$ groups is 279 pm, well below the sum of the van der Waals radii of 294 pm.

The eight atoms of the bridging groups almost lie all in the molecular pseudo mirror plane. The deviations of the atoms from their best plane are given in Table 2.

The relatively large deviation of the carbonyl carbon atom from this plane is also expressed by different distances to the iron atoms (196 and 203 pm) indicating a slight tendency to a semibridging species, which, however, is not feasible in the presence of the two symmetrically arranged $CF_2$ bridges. The angles Fe–C(O)–Fe and the Fe–C($F_2$)–Fe comprise 76.5° and 76.6°, respectively, and are closely related to those in $Fe_2(CO)_9$ with 77.6° [15].

**Table 2** Deviation of the bridging atoms in **2** from the best plane (in pm)

| | | | |
|---|---|---|---|
| C(5) | –4.14 | F(2) | +1.80 |
| O(5) | +0.92 | C(6a) | +1.81 |
| C(6) | +1.81 | F(1a) | –1.99 |
| F(1) | –1.99 | F(2a) | +1.80 |

**Table 3** Distances/pm and angles/° in **2**

| | | | |
|---|---|---|---|
| Fe(1)–C(1) | 181.4(5) | Fe(2)–C(6) | 197.6(4) |
| Fe(1)–C(2a) | 183.3(4) | Fe(2)–C(6a) | 197.6(4) |
| Fe(1)–C(2) | 183.3(4) | Fe(2)–C(5) | 202.7(6) |
| Fe(1)–C(5) | 196.1(5) | C(1)–O(1) | 112.7(7) |
| Fe(1)–C(6a) | 200.8(4) | C(2)–O(2) | 112.2(4) |
| Fe(1)–C(6) | 200.8(4) | C(3)–O(3) | 114.2(7) |
| Fe(1)–Fe(2) | 246.87(11) | C(4)–O(4) | 112.3(5) |
| Fe(2)–C(3) | 180.7(6) | C(5)–O(5) | 115.0(6) |
| Fe(2)–C(4) | 184.0(4) | C(6)–F(1) | 135.1(4) |
| Fe(2)–C(4a) | 184.0(4) | C(6)–F(2) | 135.3(4) |
| | | | |
| C(1)–Fe(1)–C(2a) | 93.51(15) | C(4)–Fe(2)–C(6) | 91.14(16) |
| C(1)–Fe(1)–C(2) | 93.51(15) | C(4a)–Fe(2)–C(6) | 170.19(16) |
| C(2a)–Fe(1)–C(2) | 97.1(2) | C(3)–Fe(2)–C(6a) | 91.38(17) |
| C(1)–Fe(1)–C(5) | 177.9(2) | C(4)–Fe(2)–C(6a) | 170.19(16) |
| C(2a)–Fe(1)–C(5) | 87.87(16) | C(4a)–Fe(2)–C(6a) | 91.14(16) |
| C(2)–Fe(1)–C(5) | 87.87(16) | C(6)–Fe(2)–C(6a) | 81.5(2) |
| C(1)–Fe(1)–C(6a) | 89.94(16) | C(3)–Fe(2)–C(5) | 178.5(2) |
| C(2a)–Fe(1)–C(6a) | 91.37(15) | C(4)–Fe(2)–C(5) | 85.66(16) |
| C(2)–Fe(1)–C(6a) | 170.66(15) | C(4a)–Fe(2)–C(5) | 85.66(16) |
| C(5)–Fe(1)–C(6a) | 88.46(17) | C(6)–Fe(2)–C(5) | 87.52(15) |
| C(1)–Fe(1)–C(6) | 89.94(16) | C(6a)–Fe(2)–C(5) | 87.52(15) |
| C(2a)–Fe(1)–C(6) | 170.67(15) | C(3)–Fe(2)–Fe(1) | 127.98(18) |
| C(2)–Fe(1)–C(6) | 91.37(15) | C(4)–Fe(2)–Fe(1) | 117.95(12) |
| C(5)–Fe(1)–C(6) | 88.46(17) | C(4a)–Fe(2)–Fe(1) | 117.95(12) |
| C(6a)–Fe(1)–C(6) | 79.9(2) | C(6)–Fe(2)–Fe(1) | 52.30(10) |
| C(1)–Fe(1)–Fe(2) | 124.94(16) | C(6a)–Fe(2)–Fe(1) | 52.30(10) |
| C(2a)–Fe(1)–Fe(2) | 120.36(11) | C(5)–Fe(2)–Fe(1) | 50.57(15) |
| C(2)–Fe(1)–Fe(2) | 120.36(11) | O(1)–C(1)–Fe(1) | 179.0(3) |
| C(5)–Fe(1)–Fe(2) | 52.98(17) | O(2)–C(2)–Fe(1) | 178.6(3) |
| C(6a)–Fe(1)–Fe(2) | 51.12(10) | O(3)–C(3)–Fe(2) | 178.6(5) |
| C(6)–Fe(1)–Fe(2) | 51.12(10) | O(4)–C(4)–Fe(2) | 178.4(4) |
| C(3)–Fe(2)–C(4) | 95.3(17) | O(5)–C(5)–Fe(1) | 145.0(5) |
| C(3)–Fe(2)–C(4a) | 95.3(17) | O(5)–C(5)–Fe(2) | 138.5(5) |
| C(4)–Fe(2)–C(4a) | 95.4(2) | Fe(1)–C(5)–Fe(2) | 76.5(2) |
| C(3)–Fe(2)–C(6) | 91.38(17) | Fe(2)–C(6)–Fe(1) | 76.58(12) |
| F(2)–C(6)–F(1) | 103.0(3) | F(2)–C(6)–Fe(2) | 119.4(3) |
| F(1)–C(6)–Fe(2) | 120.5(2) | F(2)–C(6)–Fe(1) | 118.7(2) |
| F(1)–C(6)–Fe(1) | 118.4(2) | | |

### *3.3 Molecular structure of **3***

The crystal structure of **3** shows an unusual elongation of the thermal ellipsoids of the iron atoms perpendicular to the crystallographic mirror plane as well as a similar elongation with the bridging carbonyl carbon atoms parallel to this plane as depicted in Fig. 2. The latter features are independent from the absorption correction and from the data collection technique. In fact, the data were measured twice on different diffractometers having different diffraction geometries. Moreover, merohedral twinning can be excluded on the basis of the crystal's metrics and as in the diffraction pattern of the IPDS measurement there were no signs of additional individuals which could suggest a non-merohedral twin. Ultimatively, it may be reasonably hypothesized that **3** is an average structure from two less symmetric species, namely it results from the superposition of the enantiomers **3a** and **3b** with two semibridging CO ligands in place of the symmetrically bridging ones as represented in Fig. 3. Thus, **3** can be considered as the racemic mixture. Calculation of a split model for all atoms except O(5) and C(6) improved considerably the quality of the refinement and the plausibility of the thermal ellipsoids. We also restrained all of the terminal Fe–C and C–O distances as well as the C–F ones to be consistently equal (See table 4).

The enantiomers **3a** and **3b** can be considered as intermediates on the way from a singly bridged structure as proposed for $Os_2(CO)_9$ to the triply bridged structure recorded for $Fe_2(CO)_9$. The lack of clear bridging $\nu$(CO) vibrations in the IR spectrum, as in contrast recorded for **2**, supports this view.

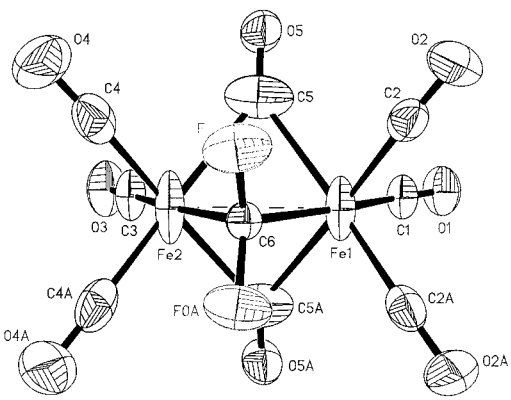


**Fig. 2** Crystal structure of **3,** average structure; with atomic numbering scheme; thermal ellipsoids are shown at the 50% probability level.

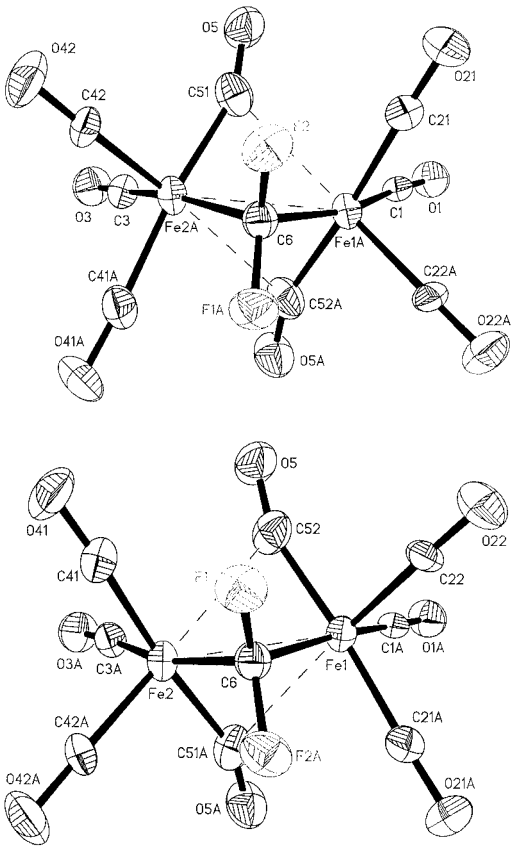


**Fig. 3** Crystal structures of the separated enantiomers **3a** and **3b**; with atomic numbering scheme; thermal ellipsoids are shown at the 50% probability level.

The most dramatic effect on dealing with the enantiomers **3a** and **3b** concerns the two possible angles O(5)–C(5)–Fe(1) which, from the unique 144° in the average structure **3**, become very different. Thus, O(5)–C(5)–Fe(1) is as close as 129° (semibridging mode) and O(5)–C(5)–Fe(2) is as open as 160° (terminal mode). Also, the unusually long Fe–C(5) average distances of 215 pm observed in **3** subdivides into a short (183 pm) and long (249 pm) separation to the first and the second iron atom, respectively. This separation also causes the Fe–Fe distance to elongate slightly from 254 pm in **3** into 258 pm in **3a** and **3b**. With respect to **2** the Fe–C($F_2$)–Fe angle has increased to 80° (**3**) or 81° (**3a, b**). In Table 4 distances and angles of the average and the separated structures are compared. The structural parameters for the semibridging CO groups in **3a** or **3b** are consistent with those found in [Cp(CO)Fe($\mu$-CO)($\mu$-$CF_2$)IrCl(CO)-($PMe_2Ph$)]$BF_4$ [14], and $Fe_2(CO)_7$dipy [16] which contain clearly defined semibridging CO groups. In the latter, however, the groups connect different metal atoms or metal atoms with different substituents. Semibridging CO groups serve to remove electron density from the more negatively charged part of the molecule and are not found in dinuclear compounds with two identical molecule halves [16].

**Table 4** Distances/pm and angles/° in **3** and in **3a, b**

| average structure of **3** | | disordered structure **3a, b** | |
|---|---|---|---|
| Fe(1)–C(2) | 181.0(4) | Fe(1)–C(21a) | 180.8(6) |
| Fe(1)–C(1) | 183.6(4) | Fe(1)–C(1a) | 183.6(2) |
| Fe(1)–C(6) | 197.6(4) | Fe(1)–C(6) | 198.69(17) |
| Fe(1)–C(5) | 215.2(5) | Fe(1)–C(51a), | 246.1(6), |
| | | Fe(1)–C(52) | 184.8(6) |
| Fe(1)–Fe(2) | 254.05(9) | Fe(1)–Fe(2) | 258.16(6) |
| Fe(2)–C(4) | 181.7(5) | Fe(2)–C(42a) | 180.2(5) |
| Fe(2)–C(3) | 183.4(5) | Fe(2)–C(3a) | 183.4(3) |
| Fe(2)–C(6) | 197.3(4) | Fe(2)–C(6) | 198.75(19) |
| Fe(2)–C(5) | 215.3(5) | Fe(2)–C(52), | 248.9(6), |
| | | Fe(2)–C(51a) | 183.0(6) |
| C(1)–O(1) | 112.7(5) | C(1a)–O(1a) | 112.9(3) |
| C(2)–O(2) | 112.8(6) | C(21a)–O(21a), | 114.9(5), |
| | | C(22)–O(22) | 114.1(5) |
| C(3)–O(3) | 113.3(5) | C(3a)–O(3a) | 113.3(3) |
| C(4)–O(4) | 113.1(5) | C(41)–O(41), | 114.8(5), |
| | | C(42)–O(42) | 115.0(5) |
| C(6)–F | 135.5(3) | C(6)–F(1), | 136.7(4), |
| | | C(6)–F(2a) | 137.0(4) |
| C(5)–O(5) | 109.1(5) | C(51a)–O(5a), | 111.8(6), |
| | | C(52)–O(5) | 112.3(6) |
| C(2)–Fe(1)–C(2a) | 94.2(2) | C(21a)–Fe(1)–C(22) | 94.3(7) |
| C(2)–Fe(1)–C(1) | 95.71(14) | C(21a)–Fe(1)–C(1a) | 92.1(8) |
| C(2)–Fe(1)–C(6) | 91.35(13) | C(21a)–Fe(1)–C(6) | 87.7(6) |
| C(1)–Fe(1)–C(6) | 169.62(18) | C(1a)–Fe(1)–C(6) | 166.8(4) |
| C(2)–Fe(1)–C(5) | 85.11(17) | C(21a)–Fe(1)–C(51a) | 79.4(7) |
| C(2a)–Fe(1)–C(5) | 173.95(16) | C(22)–Fe(1)–C(51a) | 167.6(7) |
| C(1)–Fe(1)–C(5) | 90.35(15) | C(1a)–Fe(1)–C(51a) | 92.1(5) |
| C(6)–Fe(1)–C(5) | 82.66(14) | C(6)–Fe(1)–C(51a) | 74.86(12) |
| C(5)–Fe(1)–C(5a) | 95.0(3) | C(52)–Fe(1)–C(51a) | 95.6(2) |
| C(2)–Fe(1)–Fe(2) | 122.39(10) | C(22)–Fe(1)–Fe(2), | 133.2(5) |
| | | C(21a)–Fe(1)–Fe(2) | 110.0(4) |
| C(1)–Fe(1)–Fe(2) | 119.71(13) | C(1a)–Fe(1)–Fe(2) | 118.7(7) |
| C(6)–Fe(1)–Fe(2) | 49.91(12) | C(6)–Fe(1)–Fe(2) | 49.5(2) |
| C(5)–Fe(1)–Fe(2) | 53.84(14) | C(52)–Fe(1)–Fe(2), | 66.0(2) |
| | | C(51a)–Fe(1)–Fe(2) | 42.5(2) |
| C(4)–Fe(2)–C(4a) | 95.1(2) | C(41)–Fe(2)–C(42a) | 95.4(3) |
| C(4)–Fe(2)–C(3) | 95.87(15) | C(42a)–Fe(2)–C(3a) | 99.3(6) |
| C(4)–Fe(2)–C(6) | 91.72(13) | C(4a)–Fe(2)–C(6) | 95.7(6) |
| C(3)–Fe(2)–C(6) | 168.75(18) | C(3a)–Fe(2)–C(6) | 165.0(4) |
| C(4)–Fe(2)–C(5) | 84.73(17) | C(41)–Fe(2)–C(52), | 95.5(8) |
| | | C(42a)–Fe(2)–C(51a) | 91.0(7) |
| C(4a)–Fe(2)–C(5) | 174.42(17) | C(42a)–Fe(2)–C(52), | 168.8(5) |
| | | C(41)–Fe(2)–C(51a) | 173.5(4) |
| C(3)–Fe(2)–C(5) | 89.69(15) | C(3a)–Fe(2)–C(52), | 90.3(5) |
| | | C(3a)–Fe(2)–C(51a) | 88.4(7) |
| C(6)–Fe(2)–C(5) | 82.72(14) | C(6)–Fe(2)–C(52) | 74.8(2) |
| C(5)–Fe(2)–C(5a) | 94.9(3) | | |
| C(4)–Fe(2)–Fe(1) | 122.42(11) | | |
| C(3)–Fe(2)–Fe(1) | 118.73(14) | | |
| C(6)–Fe(2)–Fe(1) | 50.02(11) | C(6)–Fe(2)–Fe(1) | 49.5(2) |
| C(5)–Fe(2)–Fe(1) | 55.83(14) | C(52)–Fe(2)–Fe(1), | 42.7(8), |
| | | C(51a)–Fe(2)–Fe(1) | 65.2(6) |
| O(1)–C(1)–Fe(1) | 175.5(4) | O(1a)–C(1a)–Fe(1) | 175.3(6) |
| O(3)–C(3)–Fe(2) | 177.1(4) | O(3a)–C(3a)–Fe(2) | 175.6(4) |
| O(2)–C(2)–Fe(1) | 177.8(3) | O(21a)–C(21a)–Fe(1) | 177.9(19) |
| O(4)–C(4)–Fe(2) | 178.7(4) | O(42a)–C(42a)–Fe(2) | 178.0(13) |
| F–C(6)–F(a) | 100.9(3) | F(1)–C(6)–F(2a) | 102.1(4) |
| F–C(6)–Fe(2) | 119.3(2) | F(1)–C(6)–Fe(2), | 119.9(4), |
| | | F(2a)–C(6)–Fe(2) | 117.2(4) |
| F–C(6)–Fe(1) | 119.06(19) | F(1)–C(6)–Fe(1), | 119.4(4), |
| | | F(2a)–C(6)–Fe(1) | 117.7(3) |
| Fe(2)–C(6)–Fe(1) | 80.07(15) | Fe(2)–C(6)–Fe(1) | 81.01(7) |
| O(5)–C(5)–Fe(1) | 144.1(4) | O(5a)–C(51a)–Fe(1), | 129.4(3) |
| | | O(5a)–C(51a)–Fe(2) | 158.1(3) |
| O(5)–C(5)–Fe(2) | 143.4(5) | O(5)–C(52)–Fe(2), | 128.7(7) |
| | | O(5)–C(52)–Fe(1) | 160.0(4) |
| Fe(1)–C(5)–Fe(2) | 72.33(14) | Fe(1)–C(52)–Fe(2), | 71.3(2) |
| | | Fe(1)–C(51a)–Fe(2) | 72.3(2) |

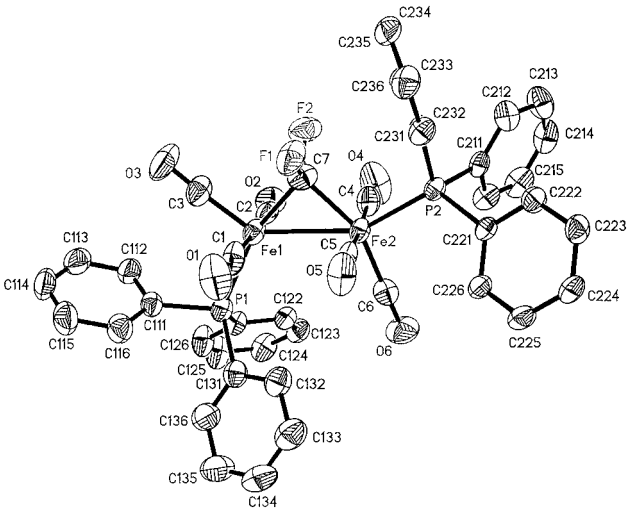


**Fig. 4** Crystal structure of **4**; with atomic numbering scheme; thermal ellipsoids are shown at the 50% probability level.

### *3.4 Molecular structure of **4***

The replacement of two terminal CO groups in **2** by $PPh_3$ affects the molecular structure dramatically as depicted in Fig. 4. The remaining six CO groups are now bonded in a terminal manner and the structure can be viewed as derived from the structure proposed for $Os_2(CO)_9$ [15] which carries only one CO bridge. The crystal structure of **4** is the first example of a compound where a $CF_2$ bridge is not accompanied by an additional bridging group. The Fe–Fe distance has increased to a value similar to that found in $[Fe_2(CO)_8]^{2-}$ [17] and in $Fe_2(CO)_8(\mu\text{-}E)$ compounds with a single bridging ligand (E = C=$CF_2$, 268 pm [18]; E = $SiR_2$, 272 pm [19]). Probably for sterical reasons, the two $PPh_3$ groups are not arranged symmetrically; one is in *cis* position and the other one in *trans* position to the bridging $CF_2$ ligand.

The Fe(1)–C(7)–Fe(2) angle at the $CF_2$ ligand is more open than in **2** and **3**, and is similar to the related angle in compounds such as $Fe_2(CO)_7\{(Ph_2P)_2CH_2\}$ with a single carbonyl bridge [20]. This emphasizes the similar behavior of CO and $CF_2$ ligands.

In comparison to olefine complexes the structure of **4** can also be viewed as a coordination of the carbene complex $Ph_3P(CO)_3Fe{=}CF_2$ with its double bond in the equatorial position of the 16 electron fragment $Ph_3P(CO)_3Fe$. Also the formulation of **4** as a bis-ferracyclopropane could be possibly taken into account.

## 4 Theoretical Analysis

In this section we discuss the alteration of the electronic, structural and bonding properties caused by the stepwise replacement of bridging CO by $CF_2$ groups in diiron carbonyls. To get a deeper insight into what happens, we consider not only difluormethylene but involve also the parent methylene $CH_2$ (see Scheme 1). The analysis is closely related to that given recently for bridging alkylindium(I) groups [21].

**Table 5** Distances/pm and angles/° in **4**

| | | | |
|---|---|---|---|
| Fe(1)–C(3) | 175.5(6) | P(1)–C(131) | 184.0(2) |
| Fe(1)–C(1) | 179.6(5) | P(2)–C(231) | 184.31(19) |
| Fe(1)–C(2) | 179.7(4) | P(2)–C(221) | 184.33(17) |
| Fe(1)–C(7) | 198.4(4) | P(2)–C(211) | 184.64(19) |
| Fe(1)–P(1) | 230.89(11) | C(1)–O(1) | 114.9(5) |
| Fe(1)–Fe(2) | 270.65(11) | C(2)–O(2) | 115.9(5) |
| Fe(2)–C(6) | 179.3(4) | C(3)–O(3) | 115.1(5) |
| Fe(2)–C(5) | 179.4(4) | C(4)–O(4) | 115.1(5) |
| Fe(2)–C(4) | 179.9(4) | C(5)–O(5) | 114.6(4) |
| Fe(2)–C(7) | 197.4(5) | C(6)–O(6) | 114.7(5) |
| Fe(2)–P(2) | 223.53(11) | C(7)–F(1) | 137.8(4) |
| P(1)–C(121) | 183.5(2) | C(7)–F(2) | 139.1(5) |
| P(1)–C(111) | 183.7(2) | | |
| C(3)–Fe(1)–C(1) | 90.4(2) | C(6)–Fe(2)–C(5) | 94.18(17) |
| C(3)–Fe(1)–C(2) | 88.1(2) | C(6)–Fe(2)–C(4) | 91.32(19) |
| C(1)–Fe(1)–C(2) | 173.09(18) | C(5)–Fe(2)–C(4) | 174.5(2) |
| C(3)–Fe(1)–C(7) | 95.0(2) | C(6)–Fe(2)–C(7) | 154.37(18) |
| C(1)–Fe(1)–C(7) | 93.05(18) | C(5)–Fe(2)–C(7) | 87.47(17) |
| C(2)–Fe(1)–C(7) | 93.81(17) | C(4)–Fe(2)–C(7) | 87.29(19) |
| C(3)–Fe(1)–P(1) | 102.24(15) | C(6)–Fe(2)–P(2) | 102.56(13) |
| C(1)–Fe(1)–P(1) | 84.85(14) | C(5)–Fe(2)–P(2) | 88.05(13) |
| C(2)–Fe(1)–P(1) | 88.87(12) | C(4)–Fe(2)–P(2) | 91.39(14) |
| C(7)–Fe(1)–P(1) | 162.66(13) | C(7)–Fe(2)–P(2) | 103.06(12) |
| C(3)–Fe(1)–Fe(2) | 141.43(14) | C(6)–Fe(2)–Fe(1) | 107.44(13) |
| C(1)–Fe(1)–Fe(2) | 95.23(14) | C(5)–Fe(2)–Fe(1) | 87.73(13) |
| C(2)–Fe(1)–Fe(2) | 90.13(13) | C(4)–Fe(2)–Fe(1) | 90.01(14) |
| C(7)–Fe(1)–Fe(2) | 46.71(13) | C(7)–Fe(2)–Fe(1) | 47.00(12) |
| P(1)–Fe(1)–Fe(2) | 116.24(4) | P(2)–Fe(2)–Fe(1) | 149.92(4) |
| O(1)–C(1)–Fe(1) | 173.6(4) | F(1)–C(7)–F(2) | 101.2(3) |
| O(2)–C(2)–Fe(1) | 173.9(4) | F(1)–C(7)–Fe(2) | 118.6(3) |
| O(3)–C(3)–Fe(1) | 177.3(4) | F(2)–C(7)–Fe(2) | 119.0(3) |
| O(4)–C(4)–Fe(2) | 177.2(4) | F(1)–C(7)–Fe(1) | 116.2(3) |
| O(5)–C(5)–Fe(2) | 176.6(3) | F(2)–C(7)–Fe(1) | 116.4(3) |
| O(6)–C(6)–Fe(2) | 179.1(4) | Fe(2)–C(7)–Fe(1) | 86.29(16) |

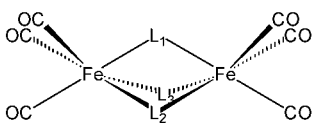


**Scheme 2**

Density functional theory (DFT) optimizations applying the B3LYP functionals [22] were performed using the Gaussian98 package [23]. Effective core potentials with Ne core in connection with the corresponding valence basis set was employed for Fe [24], whereas the standard 6-31G* basis set was used for the other atoms. The optimizations were carried out keeping certain symmetries for the structures. For n = 0 and n = 3, this is $D_{3h}$ symmetry. For n = 1 and n = 2, we used $C_{2v}$ symmetry. The optimized structures for the cases n = 2 and n = 3 are determined as minima on the potential surface. In the cases n = 1, frequency calculations yield an imaginary frequency of 94i and 108i for L = $CF_2$ and L = $CH_2$, respectively. The vibration corresponding to the imaginary frequency indicates an asymmetric distortion of the two bridging carbonyl ligands. Geometry optimizations of

these systems in lower symmetry lead to singly bridged structures. Otherwise, the experiments indicate the semibridged structure **3 a, b** for $L = CF_2$ and a symmetrically triple-bridged structure for $L = CH_2$ [25]. In agreement with the strategy used in ref. [21], we consider in the following only symmetrically triple-bridged systems for the sake of systematic and direct comparisons within the series from $n = 0$ to $n = 3$. Thus, for $n = 1$ with $L = CF_2$, we refer to the average structure **3** instead of the disordered structure **3 a, b** (Table 4).

Selected structural parameters resulting from the geometry optimizations are presented in Table 6 and Table 7 for $L = CF_2$ and $L = CH_2$, respectively. The experimental values available are given in parenthesis. The agreement appears generally good. Opposite to the trend found for InR substitution in $Fe_2(CO)_9$ [21], there is a systematic *decrease* of the Fe–Fe distance in going from $n = 0$ to $n = 3$. This effect is significantly stronger for $CH_2$ than for $CF_2$. Since the metal-bridge distances remain nearly constant, the angles at the bridges decrease correspondingly. For both the $CF_2$ and the $CH_2$ substitutions, the calculated terminal bond distances (Fe–C as well as C–O) do not change significantly within the series.

In order to find out the electronic reasons for the structural peculiarities pointed out, a natural bond order (NBO) population analysis [26] was performed. In Tables 8 and 9, selected population values are collected. The total populations at the bridges are separated into a $\sigma$ and a $\pi$ part (given in brackets). Only the contributions of the $p_\pi$ atomic orbitals (AOs) *out of* the plane of the bridging ligands are involved in the backbonding and are, therefore, included into the $\pi$ part. The latter is contributed from all of the AOs of the bridging CO and $CF_2$ ligands, whereas a single carbon $p_\pi$ orbital is involved in case of $CH_2$. The contributions from the remaining AOs are all collected in the $\sigma$ part, including the CO $p_\pi$ orbitals lying *in* the plane of the bridging ligands.

In both series, the population at the iron centers decreases in going from $n = 0$ to $n = 3$. The same applies to the terminal carbonyl ligands as well. Consequently, the total population of the bridging system increases (as referred to the standard populations). However, the distinction between the $\sigma$ and $\pi$ populations of the bridges indicate that their $\pi$ acceptor capability is exerted more efficiently than the $\sigma$ donor one. Thus, in going from $n = 0$ to $n = 3$, the bridging moiety receives more electron density from the metals than it transfers to them. It turns out that these charge transfer effects are stronger for $CH_2$ than for $CF_2$ substitu-

**Table 6** Selected Structural Parameters (pm, deg) for $(CO)_3Fe(\mu\text{-}CO)_{3-n}(\mu\text{-}CF_2)_nFe(CO)_3$ (n = 0, 1, 2, 3)[a,b]

| | n = 0 | n = 1 | n = 2 | n = 3 |
|---|---|---|---|---|
| Fe–Fe | 252.6 *(252.3)* | 251.5 *(254.1)* | 249.8 *(246.9)* | 248.2 |
| $Fe–C_{br}(O)$ | 200.8 *(201.6)* | 200.7 *(215.3)* | 200.8 *(199.5)* | |
| $Fe–C_{br}(F)$ | | 201.1 *(197.5)* | 201.0 *(199.1)* | 201.4 |
| C–O | 117.0 *(117.6)* | 116.7 *(109,1)* | 116.6 *(115.0)* | |
| C–F | | 135.8 *(135.5)* | 135.5 *(135.2)* | 135.2 |
| $Fe–C_{term}$ | 181.6 *(183.8)* | 181.5/*(182.1)* | 181.5/*(182.8)* | 181.4 |
| $C_{term}–O_{term}$ | 114.7 *(115.6)* | 114.6/*(113.0)* | 114.5/*(112.9)* | 114.5 |
| $Fe–C_{br}(O)–Fe$ | 79.0 *(77.6)* | 77.4 *(72.3)* | 76.8 *(76.5)* | |
| $Fe–C_{br}(F)–Fe$ | | 77.6 *(80.1)* | 77.0 *(76.6)* | 76.1 |

[a] Averaged values for $n = 1$ and $n = 2$. [b] Experimental values (in parenthesis) from ref. [15] ($n = 0$), from the average structure of **3** in Table 4 ($n = 1$) and from Table 3 ($n = 2$).

**Table 7** Selected Structural Parameters (pm, deg) for $(CO)_3Fe(\mu\text{-}CO)_{3-n}(\mu\text{-}CH_2)_nFe(CO)_3$ (n = 0, 1, 2, 3)[a,b]

| | n = 0 | n = 1 | n = 2 | n = 3 |
|---|---|---|---|---|
| Fe–Fe | 252.6 *(252.3)* | 250.4 *(250.4)* | 246.3 | 241.0 |
| $Fe–C_{br}(O)$ | 200.8 *(201.6)* | 200.7 *(201.5)* | 201.0 | |
| $Fe–C_{br}(H)$ | | 202.2 *(201.5)* | 201.3 | 200.7 |
| C–O | 117.0 *(117.6)* | 116.8 | 116.4 | |
| C–H | | 109.2 | 109.2 | 109.2 |
| $Fe–C_{term}$ | 181.6 *(183.8)* | 180.8 *(182.3)* | 181.1/177.9 | 180.2 |
| $C_{term}–O_{term}$ | 114.7 *(115.6)* | 114.8 | 114.8 | 114.9 |
| $Fe–C_{br}(O)–Fe$ | 79.0 *(77.6)* | 77.2 *(76.6)* | 75.6 | |
| $Fe–C_{br}(H)–Fe$ | | 76.5 *(76.6)* | 75.4 | 73.8 |

[a] Averaged values for $n = 1$ and $n = 2$. [b] Experimental values (in parenthesis) from ref. [15] ($n = 0$) and from ref. [25] ($n = 1$).

**Table 8** NBO Population Values for $(CO)_3Fe(\mu\text{-}CO)_{3-n}(\mu\text{-}CF_2)_nFe(CO)_3$ (n = 0, 1, 2, 3)[a,b,c]

| | n = 0 | n = 1 | n = 2 | n = 3 |
|---|---|---|---|---|
| Fe | 16.577 | 16.563 | 16.549 | 16.533 |
| $CF_2$ | | 24.112 | 24.099 | 24.075 |
| | | *(19.361/4.751)* | *(19.369/4.730)* | *(19.384/4.691)* |
| $CO_{br}$ | 13.985 | 13.972 | 13.951 | |
| | *(11.532/2.453)* | *(11.518/2.454)* | *(11.529/2.422)* | |
| $\Sigma$bridges | 41.955 | 52.056 | *62.149* | 72.225 |
| | *(34.596/7.359)* | *(42.397/9.659)* | *(50.267/11.882)* | *(58.152/14.073)* |
| $\Delta\Sigma$bridges | –0.045 | 0.056 | 0.149 | 0.225 |
| | *(–1.404/1.359)* | *(–1.603/1.659)* | *(–1.733/1.882)* | *(–1.848/2.073)* |
| $CO_{term}$ | 13.815 | 13.796/13.816 | 13.803/13.772 | 13.785 |
| $\Delta CO_{term}$ | –0.185 | –0.204/–0.184 | –0.197/–0.228 | –0.215 |

[a] Averaged values for $n = 1$ and $n = 2$. [b] $\sigma$ and $\pi$ components (see text) in parenthesis. [c] The standard populations of the free fragments are: Fe: 16.000, $CF_2$: 24.000 (20.000/4.000), CO: 14.000 (12.000/2.000)

**Table 9** NBO Population Values for $(CO)_3Fe(\mu\text{-}CO)_{3-n}(\mu\text{-}CH_2)_nFe(CO)_3$ (n = 0, 1, 2, 3)[a,b,c]

| | n = 0 | n = 1 | n = 2 | n = 3 |
|---|---|---|---|---|
| Fe | 16.577 | 16.527 | 16.476 | 16.419 |
| $CH_2$ | | 8.176 | 8.166 | 8.130 |
| | | *(7.238/0.938)* | *(7.248/0.918)* | *(7.271/0.859)* |
| $CO_{br}$ | 13.985 | 13.972 | 13.938 | |
| | *(11.532/2.453)* | *(11.527/2.445)* | *(11.552/2.386)* | |
| $\Sigma$bridges | 41.955 | 36.120 | 30.270 | 24.390 |
| | *(34.596/7.359)* | *(30.292/5.828)* | *(26.048/4.222)* | *(21.813/2.577)* |
| $\Delta\Sigma$bridges | –0.045 | 0.120 | 0.270 | 0.390 |
| | *(–1.404/1.359)* | *(–1.708/1.828)* | *(–1.952/2.222)* | *(–2.187/2.577)* |
| $CO_{term}$ | 13.815 | 13.801/13.811 | 13.808/13.773 | 13.795 |
| $\Delta CO_{term}$ | –0.185 | –0.199/–0.189 | –0.192/–0.227 | –0.205 |

[a] Averaged values for $n = 1$ and $n = 2$. [b] $\sigma$ and $\pi$ components (see text) in parenthesis. [c] The standard populations of the free fragments are: Fe: 16.000, $CH_2$: 8.000 (8.000/0.000), CO: 14.000 (12.000/2.000)

ents. The order both for the $\sigma$ donor and $\pi$ acceptor abilities is $CO < CF_2 < CH_2$. This is also consistent with the $\pi$ acceptor order ($CO < CF_2$) estimated from the IR spectroscopy (see Section 2).

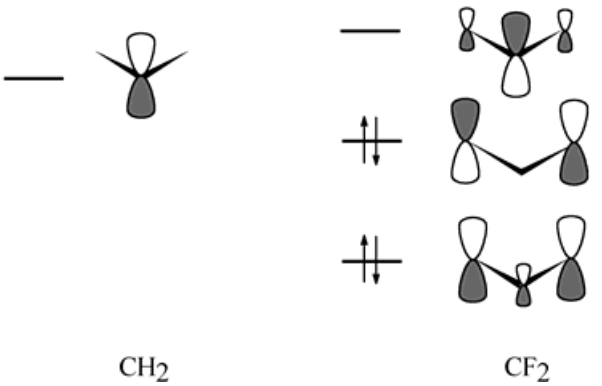


**Scheme 3**

The relations above can also be inferred from the relative energy position of the $\sigma$ donor and the $\pi$ acceptor orbitals of the free ligand molecules. The lower in energy is the MO with $\pi$ accepting capabilities, the larger is its functionality. In the case of $CH_2$, the acceptor orbital is a pure $p_\pi$ orbital located at the carbon atom. The $\pi$ electron system of $CF_2$ is of heteroallylic type (see Scheme 3), the actual acceptor MO having carbon-fluorine antibonding character. Because of the significant electronegativity difference between carbon and fluorine atoms, the latter MO receives relatively small fluorine contributions and it is only slightly destabilized compared to the pure carbon $p_\pi$ orbital of $CH_2$. The corresponding $\pi^*$ acceptor MO of CO lies highest in energy because it carries a more significant contribution from the oxygen atom. Thus, the energy order of the $\pi$ acceptor orbitals of the bridges is consistent with the different $\pi$ acceptor behavior ascertained for the dimeric complexes.


**Scheme 4**

Based on these findings, the decrease of the Fe–Fe distance within the two series can be explained. We consider the two highest occupied MOs of the symmetrically bridged complexes (e″ in $D_{3h}$, $a_2$ and $b_2$ in $C_{2v}$ symmetry). These orbitals are commonly considered to be responsible for the main part of the acceptor interaction between the bridging ligands and the metal centers. As shown Scheme 4 these levels are at the same time metal-bridge bonding and metal–metal

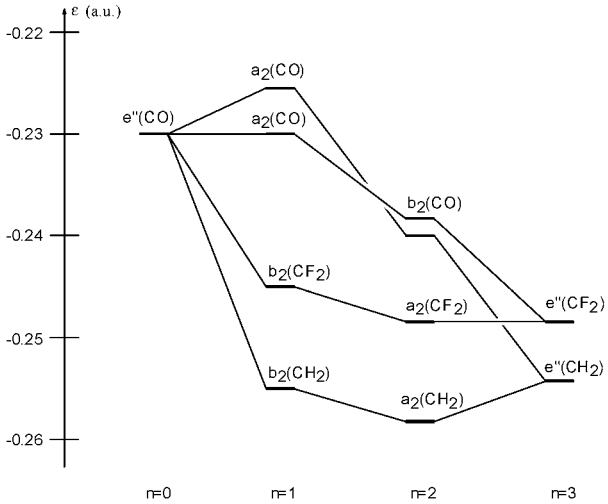


**Fig. 5** Energetic levels [a.u.] of the two highest occupied molecular orbitals for $(CO)_3Fe(\mu\text{-}CO)_{3-n}(\mu\text{-}L)_nFe(CO)_3$ ($L = CH_2$, $CF_2$; $n = 0, 1, 2, 3$)

antibonding in character. This causes a repulsive interaction between the two metal centers, as it has been pointed out before [27, 28]. In going from $n = 0$ to $n = 3$, the increase of the acceptor ability of the bridging moiety implies a decrease of electron density at the metal centers. The latter fact is attributed to the reduced iron contribution to the two highest occupied MOs. Consequently, the metal–metal antibonding character of these MOs becomes less effective. This reduces the intermetallic repulsion, which leads to a decrease of the Fe–Fe distance through the series.

In Figure 5, the energetic stabilization of the highest occupied complex MOs is shown. The MOs which describe the backdonation to $CH_2$ are the lowest in energy, those describing the interaction between CO $\pi^*$ orbitals and the iron centers are the highest. This agrees with the $\pi$ acceptor order $CO < CF_2 < CH_2$ for the individual ligands. The average of the respective orbital energies steadily decreases through the series, more so for the $CH_2$ than for $CF_2$ bridges.

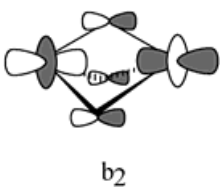


**Scheme 5**

Based on the above considerations, the decrease of the Fe–Fe distance could be ascribed mainly to the orbital interactions represented by the two highest occupied MOs. However, it is also interesting to check if qualitative MO theory and the fragment molecular orbital (FMO) analysis can add anything to our understanding of the experimental and DFT trends. To the

purpose, we have exploited the EHMO method and graphic capabilities of the CACAO package [29]. For instance, molecular orbital overlap population (MOOP) diagrams are very useful to see how the strength of a certain bond (e. g. Fe–Fe) builds up by populating progressively the MOs up to the HOMOs. From a comparison of the three different $D_{3h}$ systems with n = 3 and a fixed Fe–Fe distance of 260 pm, it is confirmed that the Fe–Fe bond strength decreases dramatically when the HOMOs are populated. Thus, the final Fe–Fe overlap population is close to zero, *i.e.*: +0.08, +0.03 and –0.03 for the $CH_2$, $CF_2$, and CO systems, respectively. The latter values, however, cannot be justified only in terms of the different Fe–Fe repulsion implicit in the HOMOs. In fact, the given trends exist already before the HOMOs are populated and their origin is attributable to another critical backdonation, namely that between the out-of-phase combination of $z^2$ orbitals and the $a_2''$ combination of $\pi$ acceptor orbitals at the bridges (see Scheme 5). In previous articles concerning $Fe_2(CO)_9$ [28], it was stated that the latter interaction is critically small but essential to admit the existence of a direct metal-metal bond. With the $CF_2$ and $CH_2$ ligands, the energy gap between the two interacting $a_2''$ FMOs is progressively reduced. Accordingly, the overlap population between the latter increases in the order $CO < CF_2 < CH_2$ (0.13, 0.17 and 0.23, respectively). By contrast, the overlap population of $a_2''$ type almost vanishes in the analogous system with three bridging InR groups [21] due to the significant electropositivity of the indium atoms. In this case, not only the metal-bridge bonding is weakened but also the impossibility for the $z^2$ orbitals to discard part of their electron density into the bridges keeps the repulsion between the metals high; in this manner, the long Fe–Fe separation of ca. 300 pm can be rationalized.

In conclusion, the comparison between systems which contain two terminal $Fe(CO)_3$ fragments and three bridging groups of different nature nicely confirms the idea that direct metal–metal bonding builds up from several different components.

## 5 Experimental Section

**General Considerations.** All operations were carried out under an argon atmosphere in dried and degassed solvents using Schlenk techniques. IR spectra (in Nujol) were run on a Nicolet 510 spectrometer. $^{13}C$ NMR spectra were recorded on a Bruker AC 300 instrument using $SiMe_4$ ($\delta = 0.00$ ppm) as the external standard. $^{19}F$ NMR and $^{31}P$ NMR spectra were run on a Bruker ARX 200 spectrometer. Mass spectra were obtained with a CH 7 instrument from MAT (Bremen). Elemental analyses were performed by the analytical service of the Fachbereich Chemie der Universität Marburg (Germany). Comercial available $Na_2[Fe(CO)_4] \cdot 1.5$ dioxane (Collman's reagent, Aldrich) and $Br_2CF_2$ (ABCR) were used without further purification. $Na_2[Fe_2(CO)_8]$ was prepared by addition of $Fe(CO)_5$ to a suspension of Collman's reagent in THF.

**Reaction of $Na_2[Fe(CO)_4] \cdot 1.5$ dioxane with $Br_2CF_2$:** A suspension of 2.00 g $Na_2[Fe(CO)_4] \cdot 1.5$ dioxane (5.80 mmol) in about 40 ml n-pentane was cooled to 0 °C. To this mixture excess $Br_2CF_2$ (1 ml) was added under vigorous stirring. After stirring for 1 h at 0 °C and an additional h at room temperature the mixture was filtered and the solution evaporated to dryness. The reaction tube with the residue was attached to a vacuum line and all volatile material was sublimed at room temperature/$10^{-3}$ torr into a Schlenck tube, which was cooled with liquid air. After 3 h 250 mg of a mixture of **2** and **3** were obtained. From $^{19}F$ NMR spectroscopy **2** and **3** are present a 1 : 20 ratio, respectively; yield 22.5%. The yields of several runs varied between about 12 and 23%.

Crystals were grown by slow blowing argon over a surface of a n-pentane solution of the mixture of **2** and **3**. The crystals were separated mechanically.

Compound **2**: Orange red crystals.

IR (KBr, Nujol): 2097, 2064, 2041, 2021 (vs, CO), 1879 (s, $\mu$-CO), 1091 (s, $\mu$-$CF_2$), 1046 (s, $\mu$-$CF_2$), 739 (s), 720 (s), 694 (m), 627 (sh), 617 (m), 571 (s) $cm^{-1}$. $^{19}F$ NMR (toluene): $\delta = 60.82, 21.67$, $^2J_{F,F} = 30.13$ Hz. Mass spectrum (m/z): 408 [M] (5%), 380 [M–CO] (7%), 341 (4%), 329 (7%), 324 [M–3 CO] (1%), 323 (11%), 313 (6%), 296 [M–4 CO] (9%), 285 (4%), 268 [M–5 CO] (7%), 257 (6%), 240 [M–6 CO] (26%), 212 [M–7 CO] (56%), 201 (15%), 199 [$(CO)_2Fe_2CF$] (22%), 193 [$Fe_2CF_2CF$] (12%), 190 [$(CO)Fe_2CF_2$] (32%), 183 [$(CO)CFe_2CF$] (12%), 174 [$Fe_2(CF)_2$] (39%), 171 [$(CO)Fe_2CF$] (11%), 162 [$Fe_2CF_2$] (38%), 154 [$(CO)Fe(CF_2)(CFH)$] (11%), 145 [$F_2Fe(CF_2)H$] (25%), 142 (14%), 135 [$(CO)Fe(CF_2)(CH)$] (15%), 131 [$Fe_2F$] (14%), 118 [$Fe(CF)_2$] (53%), 112 [$Fe(CO)_2$, $Fe_2$] (19%), 106 [$FeCF_2$] (18%), 99 [FeC(CF)] (32%), 87 [FeCF] (40%), 84 [Fe(CO)] (45%), 81 [$CF_2CF$] (36%), 77 (30%), 75 [FeF] (30%), 68 [FeC] (100%).

Compound **3**: pale yellow crystals.
$C_9F_2Fe_2O_8$ (385.79); C 27.23 (Calcd. C, 28.02).

IR (KBr, Nujol): 2066, 2039, 2016, 1950 sh (vs, CO), 1034 (s, $CF_2$), 997 (s, $CF_2$), 700 s, 598 m, 565 s $cm^{-1}$. $^{13}C$ NMR (Toluol-$d_8$): $\delta = 218.98$ (t, $^1J_{C,F} = 383.63$ Hz), 207.44 (t, CO, $^3J_{C,F} = 4.7$ Hz). $^{19}F$ NMR (Toluol-$d_8$): $\delta = 50.60$ (s). Mass spectrum (m/z): 386 [M] (2%), 370 [M–O] (0.5%), 358 [M–CO] (0.8%), 342 [M–CO–O] (2.1%), 330 [M–2 CO] (6%), 302 [M–3 CO] (1.3%), 274 [M–4 CO] (0.8%), 258 [M–3 CO–O] (1.4%), 246 [M–5 CO] (3.6%), 218 [M-6 CO or **1**] (18%), 207 (8.3%), 199 [**1**-F] (3.4%), 196 [$Fe(CO)_5$] (2%), 190 [M–7 CO] (33%), 188 (3.3%), 171 [**1**–CO–F] (5%), 168 [$Fe(CO)_4$] (5%), 162 [**1**–2 CO or $Fe_2$=$CF_2$] (26%), 143 [**1**–2 CO–F] (11%), 140 [$Fe(CO)_3$] (5%), 136 (4), 134 [**1**–3 CO] (3%), 131 [$(CO)_2FeF$] (7%), 127 (5%), 124 [$(CO)_2FeC$] (4%), 112 [$Fe_2$ or $Fe(CO)_2$] (16%), 106 [$FeCF_2$] (4.3%), 96 [(CO)FeC] (4%), 87 [FeCF] (11%), 85 [$F_3CO$] (24%), 84 [FeCO] (52%), 81 (31%), 75 [FeF] (8%), 68 [FeC] (91%), 66 [$F_2CO$] (6%), 56 [Fe] (100%), 47 [FCO] (10%), 44 [$CO_2$] (41%).

**Reaction of $Na_2[Fe_2(CO)_8]$ with $Br_2CF_2$:** 3.23 g $Na_2[Fe_2(CO)_8] \cdot 4$ THF (4.82 mmol) was treated in a silmilar manner as described above with excess $Br_2CF_2$ in n-pentane; yellow crystals of **3**: 220 mg (0.57 mmol); yield 12%.

**$Fe_2(CO)_6(\mu\text{-}CF_2)(PPh_3)_2$ (4):** To a solution of 410 mg **3** (1.06 mmol) in about 40 ml n-pentane at room temperature was poured a solution of 560 mg $PPh_3$ (2.14 mmol) in n-pentane. Within a few minutes brown crystals of **4** separated. The crystals of **4** were filtered through a G3 frit and dried in vacuum; yield 815 mg (90%).

$C_{43}H_{30}F_2Fe_2O_6P_2$ (854.31); C 59.67 (calcd. 60.45), H 3.76 (calcd. 3.54)%.

IR (Nujol): $\nu$(CO) = 2054 w, 2000 vs, 1987 vs, 1966 vs, 1933 vs, 1892 w, 1867 w, $\nu$(CF) = 997, 937 $cm^{-1}$. $^{13}C$ NMR (THF-$d_8$): $\delta = 216.18$ (CO), 216.40 ($CF_2$, $^1J_{C,F} = 246.5$ Hz). $^{31}P$ NMR (THF-$d_8$): $\delta = 55.75$ ($^3J_{P,F} = 8.4$ Hz). $^{19}F$ NMR (THF-$d_8$): $\delta = 41.50$.

*X-ray structural investigations*

Single crystals of the three compounds were grown as described above. A crystal of **2**, forming plates, was mounted in a glass capillary 0.3 mm ∅ with the aid of some high vacuum grease and was measured on a CAD4 Diffractometer (Enraf-Nonius) using CuK$\alpha$ radiation at room temperature. **3** and **4**, which form needles and platelets, respectively, were dipped into oil, mounted on glass threads and measured on a IPDS (Stoe) at –70 °C (**3**) and –60 °C (**4**). After data reduction all data were subjected to psiscan correction. Solution of the structures was effected by direct methods and improvement of the models was achieved by successive refinement cycles and difference Fourier syntheses [30]. Disorder in **3** was effectively accounted for by a model with split positions for all atoms except O(5) and C(6). Details of the structures, structure solutions and convergence are shown in table 1. The crystallographic data have been deposited as supplementary publications no. CCDC-166454 (**2**), 166455 (**3a**), 166456 (**3b**), and 166457 (**4**) at the Cambridge Crystallographic Data Centre. Copies of the data can be ordered free from CCDC, 12 Union Road, Cambridge CB2 1EZ, UK (e-mail: deposit@ccdc.cam.ac.uk).

We thank the Deutsche Forschungsgemeinschaft, the Fonds der Chemischen Industrie and the Naturwissenschaftlich-Theoretisches Zentrum der Universität Leipzig for financial support. We are also grateful to the Max-Planck-Society, Munich, Germany, for financial support. A. B. thanks the Deutsche Forschungsgemeinschaft for support through the Graduate College "Physical Chemistry of Interfaces".

## References

[1] P. J. Brothers, W. R. Roper, *Chem. Rev.* **1988**, *88*, 1293.
[2] W. Schulze, H. Hartl, K. Seppelt, *Angew. Chem*. **1986**, *98*, 189; *Angew. Chem. Int. Ed. Engl*. **1986**, *25*, 185.
[3] a) F. Seel, G. V. Röschenthaler, *Z. Anorg. Allg. Chem*. **1971**, *386*, 297; b) F. Seel, G. V. Röschenthaler, *Angew. Chem*. **1970**, *82*, 182; *Angew. Chem. Int. Ed. Engl*. **1970**, *9*, 166.
[4] a) S. Koda, *Chem. Phys.* **1982**, *66*, 383; b) E. A. Carter, W. A. Goddard, III, *J Phys. Chem*. **1988**, *88*, 1752; c) F. X. Powell, D. R. Lide, Jr., *J. Chem. Phys.* **1966**, *45*, 1067. c) C. W. Mathews, *J. Chem. Phys.* **1966**, *45*, 1068.
[5] D. G. Leopold, K. K. Murray, W. C. Lineberger, *J. Chem. Phys.* **1984**, *81*, 1048.
[6] P. J. Brothers, A. K. Burrell, G. R. Clark, C. E. F. Rickard, W. R. Roper, *J. Organomet. Chem*. **1990**, *394*, 615.
[7] H. P. Fritz, W. Kornrumpf, *Z. Naturforsch*. **1981**, *36 b*, 1375.
[8] M. S. Novikov, A. F. Khlebnikov, A. Krebs, R. R. Kostikov, *Eur. J. Org. Chem*. **1998**, 133.
[9] W. Petz, F. Weller. *Book of Abstracts of the XXXIII FECHEM ICCC*; Lisboa, **1999**, 510.
[10] B. Neumüller, W. Petz, *Organometallics* **2001**, *20*, 163.
[11] C. Kötting, W. Sander, M. Senzlober, H. Bürger, *Chem. Eur. J.* **1998**, *4*, 1611.
[12] J. D. Koola, D. M. Roddick, *Organometallics* **1991**, *10*, 591.
[13] D. L. Reger, M. D. Dukes, *J. Organomet. Chem*. **1978**, *153*, 67.
[14] A. M. Crespi, M. Sabat, D. F. Shriver, *Inorg. Chem*. **1988**, *27*, 812.
[15] F. A. Cotton, J. M. Troup, *J. Chem. Soc. Dalton Trans.* **1974**, 800.
[16] a) F. A. Cotton, J. M. Troup, *J. Am. Chem. Soc*. **1974**, *96*, 1233; b) M. Dela Varga Ortiz, R. Costa, R. Reina, personal communication.
[17] a) W. Petz, F. Weller, *Z. Kristallogr*. **1997**, *212*, 157; b) H. B. Chin, M. B. Smith, R. D. Wilson, R. Bau, *J. Am. Chem. Soc.* **1974**, *96*, 5285; c) H. Deng, S. G. Shore. *Inorg. Chem.* **1992**, *31*, 2289.
[18] W. Schulze, K. Seppelt, *Inorg. Chem*. **1988**, *27*, 3872.
[19] H. Tobita, I. Shinagawa, S. Ohnuki, M. Abe, H. Izumi, H. Ogino, *J. Organomet. Chem*. **1994**, *473*, 187.
[20] F. A. Cotton, J. M. Troup, *J. Am. Chem. Soc*. **1974**, *96*, 4422.
[21] A. Barthel, C. Mealli, W. Uhl, J. Reinhold, *Organometallics* **2001**, *20,* 786.
[22] (a) A. D. Becke, *J. Chem. Phys.* **1993**, *98*, 5648; (b) C. Lee, W. Yang, R. G. Parr, *Phys. Rev.* B **1988**, *37*, 785.
[23] M. J. Frisch, G. W. Trucks, H. B. Schlegel, G. E. Scuseria, M. A. Robb, J. R. Cheeseman, V. G. Zakrzewski, J. A. Montgomery, Jr., R. E. Stratmann, J. C. Burant, S. Dapprich, J. M. Millam, A. D. Daniels, K. N. Kudin, M. C. Strain, O. Farkas, J. Tomasi, V. Barone, M. Cossi, R. Cammi, B. Mennucci, C. Pomelli, C. Adamo, S. Clifford, J. Ochterski, G. A. Petersson, P. Y. Ayala, Q. Cui, K. Morokuma, D. K. Malick, A. D. Rabuck, K. Raghavachari, J. B. Foresman, J. Cioslowski, J. V. Ortiz, B. B. Stefanov, G. Liu, A. Liashenko, P. Piskorz, I. Komaromi, R. Gomperts, R. L. Martin, D. J. Fox, T. Keith, M. A. Al-Laham, C. Y. Peng, A. Nanayakkara, C. Gonzalez, M. Challacombe, P. M. W. Gill, B. Johnson, W. Chen, M. W. Wong, J. L. Andres, C. Gonzalez, M. Head-Gordon, E. S. Replogle, J. A. Pople, *Gaussian 98, Revision A.3;* Gaussian Inc.: Pittsburgh PA, 1998.
[24] P. J. Hay, W. R. J. Wadt, *J. Chem. Phys.* **1985**, *82*, 299.
[25] (a) C. E. Sumner, P. E. Riley, R. E. Davis, R. Pettit, *J. Am. Chem. Soc.* **1980**, *102*, 1752; (b) C. E. Summer Jr., J. A. Collier, R. Pettit, *Organometallics* **1982**, *1*, 1350.
[26] E. D. Glendening, A. E. Reed, J. E. Carpenter, F. Weinhold, *NBO Version 3.1*.
[27] R. H. Summerville, R. Hoffmann, *J. Am. Chem. Soc.* **1979**, *101*, 3821.
[28] (a) C. Mealli, D. M. Proserpio, *J. Chem. Educ.* **1990**, *386*, 203; (b) J. Reinhold, E. Hunstock, C. Mealli, *New J. Chem*. **1994**, *18*, 465; (c) E. Hunstock, C. Mealli, M. J. Calhorda, J. Reinhold, *Inorg. Chem*. **1999**, *38*, 5053.
[29] (a) C. Mealli, D. M. Proserpio, *J. Chem. Educ.* **1990**, *67*, 399; (b) C. Mealli, A. Ienco, D. M. Prosperio, *Book of Abstracts of the XXXIII ICCC*; Florence, **1998**, 510.
[30] G. M. Sheldrick, SHELXS-97 and SHELXL-97, Programs for the Solution and Refinement of Crystal Structures, Göttingen, 1997.